

# Coastal retracking using along-track echograms and its dependency on coastal topography

Kaoru Ichikawa<sup>1</sup> and XiFeng Wang<sup>2</sup>

<sup>1</sup>Affiliation not available

<sup>2</sup>Dalian Ocean University

November 22, 2022

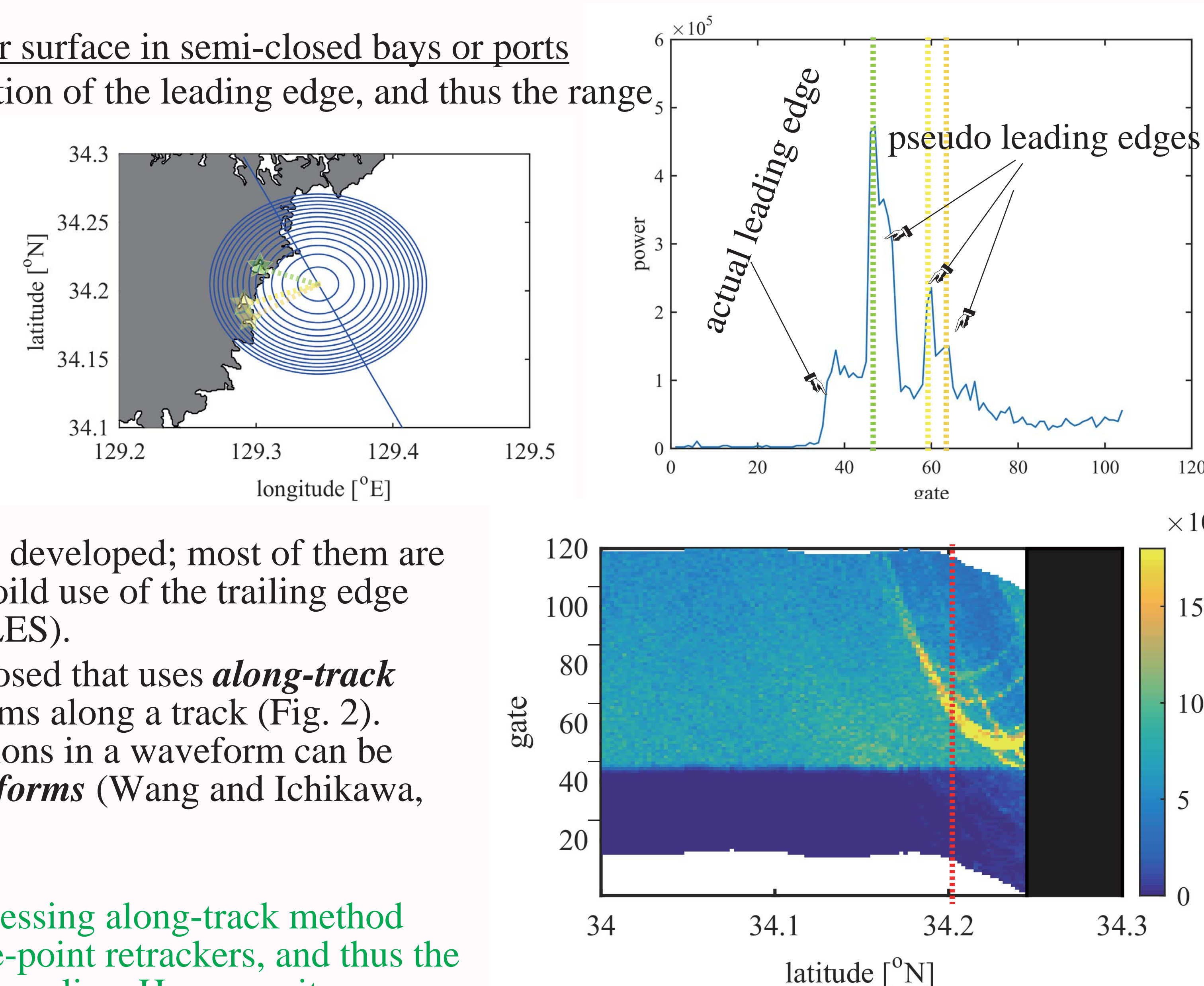
## Abstract

Although the Brown mathematical model is the standard model for waveform retracking over open oceans, coastal waveforms usually deviate from open ocean waveform shapes due to inhomogeneous surface reflections within altimeter footprints, and thus cannot be directly interpreted by the Brown model. Generally, the two primary sources of heterogeneous surface reflections are land surfaces and bright targets such as calm surface water. The former reduces echo power, while the latter often produces particularly strong echoes. In previous studies, sub-waveform retrackers, which use waveform samples collected from around leading edges in order to avoid trailing edge noise, have been recommended for coastal waveform retracking. In the present study, the peaky-type noise caused by fixed-point bright targets is explicitly detected and masked using the parabolic signature in the sequential along-track waveforms (or, azimuth-range echograms). Moreover, the power deficit of waveform trailing edges caused by weak land reflections is compensated for by estimating the ratio of sea surface area within each annular footprint in order to produce pseudo-homogeneous reflected waveforms suitable for the Brown model. Using this method, Jason-2 altimeter waveforms are retracked in several coastal areas. Our results show that both the correlation coefficient and root mean square difference between the derived sea surface height anomalies and tide gauge records retain similar values at the open ocean (0.9 and 20 cm) level, even in areas approaching 3 km from coastlines, which is considerably improved from the 10 km correlation coefficient limit of the conventional MLE4 retracker and the 7 km sub-waveform ALES retracker limit. These values, however, depend on the coastal topography of the study areas because the approach distance limit increases (decreases) in areas with complicated (straight) coastlines.

# 1. Introduction

Coastal ALT waveform (*i.e.* time-series of echo intensity) are often contaminated by  
 @weaker reflections by lands  
 @stronger reflections by calm water surface in semi-closed bays or ports  
 The latter may cause failure of detection of the leading edge, and thus the range measurements (Fig. 1).

**Fig.1** Example of contaminated waveform (right), which was measured at the location shown in the map (left). Small bays (yellow and green stars) cause pseudo leading edges in the waveform.



Several *coastal retracker*s have been developed; most of them are *sub-waveform retracker*s which avoid use of the trailing edge that might be contaminated (*e.g.* ALES).  
 In this study, a new retracker is proposed that uses *along-track echograms*, *i.e.*, sequential waveforms along a track (Fig. 2). Unlike other retracker, contaminations in a waveform can be detected by referring *neighbor waveforms* (Wang and Ichikawa, 2017).

In general, the present new post-processing along-track method performs better than the other single-point retracker, and thus the SSH can be retrieved closer to the shoreline. However, its improvement strongly depends on the coastal topography. In this presentation, the results are compared in three locations with different topography.

**Fig.2** Example of an echogram along the same track as in Fig. 1. The echo power intensity (color contours) along 34.2N (red broken line) shows the same variations as the waveform in Fig.1.

# 2. Data

The 20 Hz along-track waveform of Jason-2 in Sendor Geophysical Data Record (S-GDR) are used for Cycle 1-252 (2008.7-2015.4; AVISO).  
 For comparison, Adaptive Leading Edge Subwaveform (ALES) Jason-2 coastal altimetry product (Passaro *et al.*, 2014) are used (<http://www.coastalt.eu/community>), in addition to the traditional S-GDR retracking algorithm for open oceans.  
 Tracks #36 (across Tsushima Island, Japan) and #164 (across Taiwan) are selected for locations with different topography (Fig. 3). The area **south of Tsushima Island** (red rectangle in Fig.3) is first discussed in Section 4.1, comparing with tide gauge record at *Izuhara*. Then the **northern area** (blue rectangle) and the **south of Taiwan** (yellow rectangle) are compared in Sections 4.2 and 4.3, respectively.

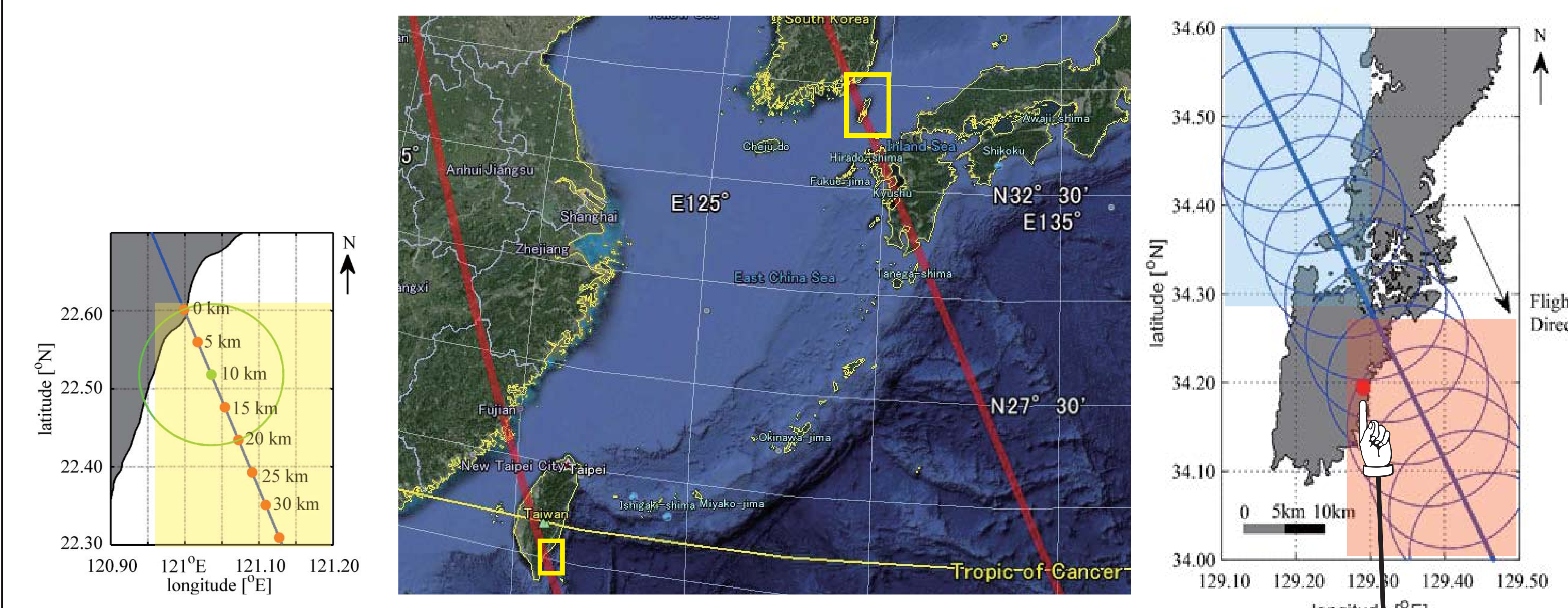


**Fig.3** Jason-2 descending tracks #36 and #164 (middle panel; Google). The track #36 passes the Tsushima Island located in the Tsushima Strait between Japan and Korea (right panel), and the track #164 passes Taiwan (left panel). Circles with the 10-km radius are plotted for reference.

# 3. Retracking Algorithms

## 3.1 Removal of bright parabolas

Since the geometry between a bright reflector on the sea surface and a satellite altimeter (Fig. 4) results in a fixed-shape parabola in the along-track echogram, the parabolic shapes are fitted recursively for all bright echos in along-track echograms. By removing these parabolas, waveforms without contaminations can be obtained, to which the theoretical Brown waveform can be fitted (Fig. 5).

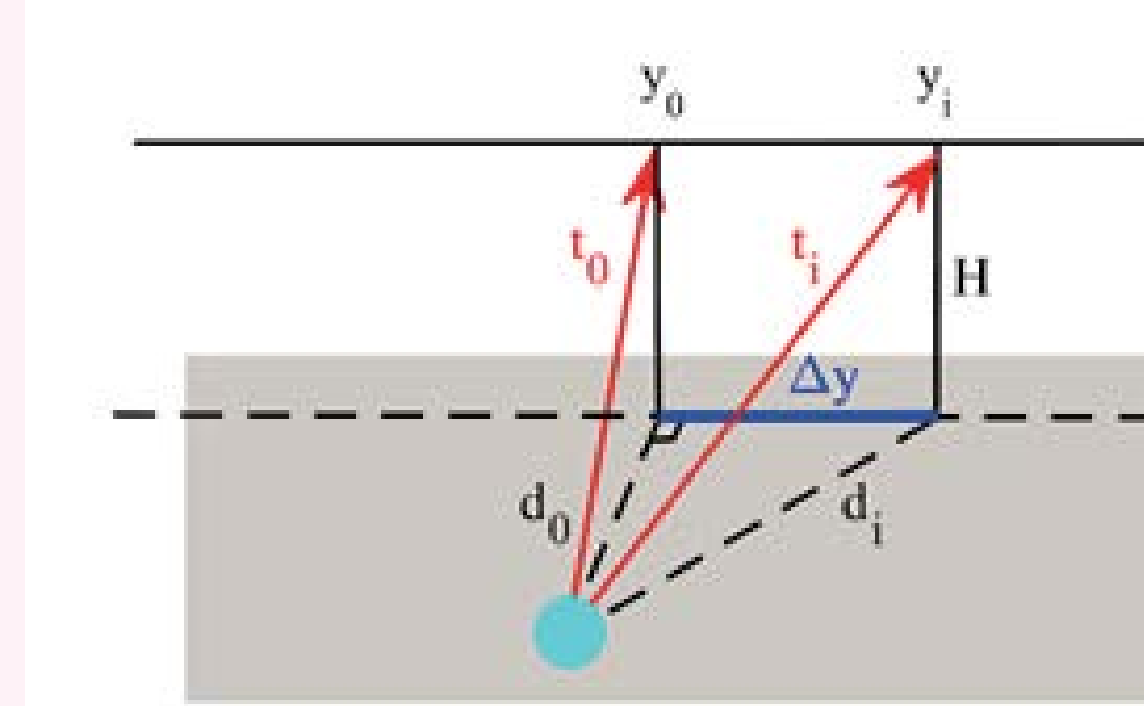


**Fig.4** Schematic showing the geometrical relationship between an altimeter and a bright reflector on the sea surface. The altimeter is closest at latitude  $y_0$  with a distance  $d_0$ .

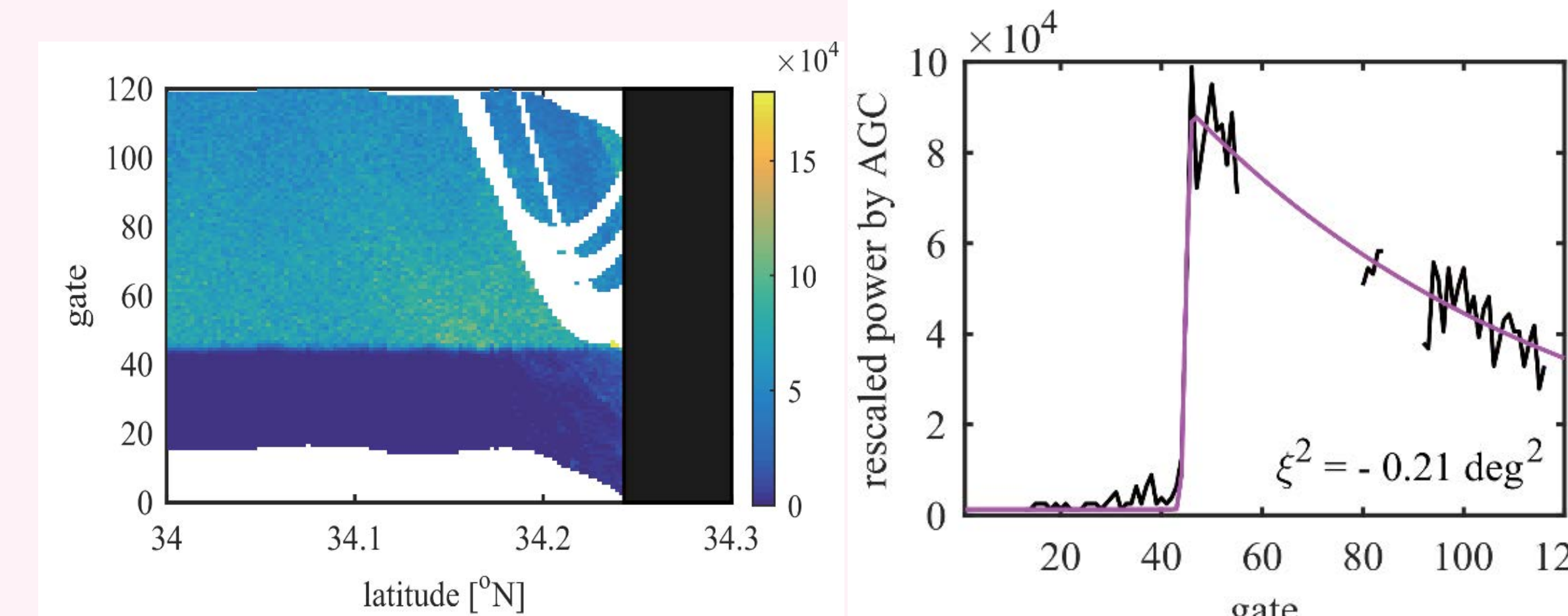


**Fig.5** The same along-track echogram in Fig.2 but after removal of the bright parabolas (left). In this case, five parabolas were removed. The waveform at 34.2N (right) contains no "pseudo leading edges" seen in Fig.1.

## 3.2 Compensation for land echo losses

Assuming that the reflected ALT signals from lands are negligible w.r.t. these from the sea, we enhance the echo intensity by the ratio of the land area in a co-range circle (Fig. 6). This procedure significantly changes the tailing edge, so that estimations of the wind speed (or sigma-0) and Significant Wave Height (SWH) are influenced. Meanwhile, its influence on the SSH is less than 10 cm in the root-mean-squared difference (RMSD).

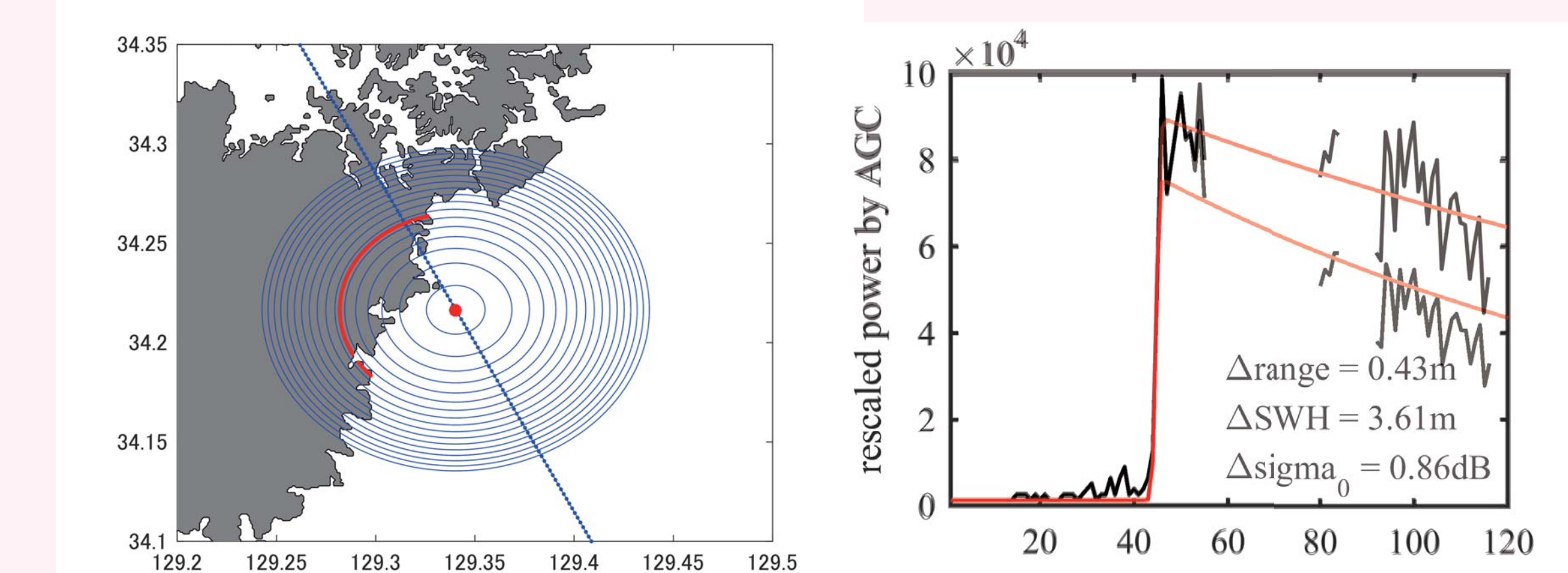


**Fig.6** Within the given co-range circle, the length ratio of the arcs over lands (red curve) is determined from the high-resolution coastline data (Wessel and Smith, 1996; left panel). The echo intensity is compensated based on this ratio (right panel). The slope of the trailing edge (*i.e.*, antenna mispointing angle) becomes small.

# 4. Area Dependency

## 4.1 South of Tsushima Island

The SSHAs from the 252-cycle mean are calculated for traditional SGDR and ALES products and for the present method. All extreme outliers (larger than 100m or smaller than -130m) are removed.

The correlation coefficient (CC) and RMSD with the tide gauge record at *Izuhara* indicate that the SSHA is available at a point **10 km** away from the shoreline for the traditional SGDR, **7 km** away for ALES and only **3 km** away for this study (Fig 7).

Time series of the SSHA at 34.21N (Fig. 8), *i.e.* 5 km away from the shoreline, shows that ALES retrieves correct SSHA, except several intermittent extreme cycles. Presence of these extreme cycles can be identified by the RMS (or, the standard deviation) of the SSHA at a point, which is used as a simple performance index in the next subsections.

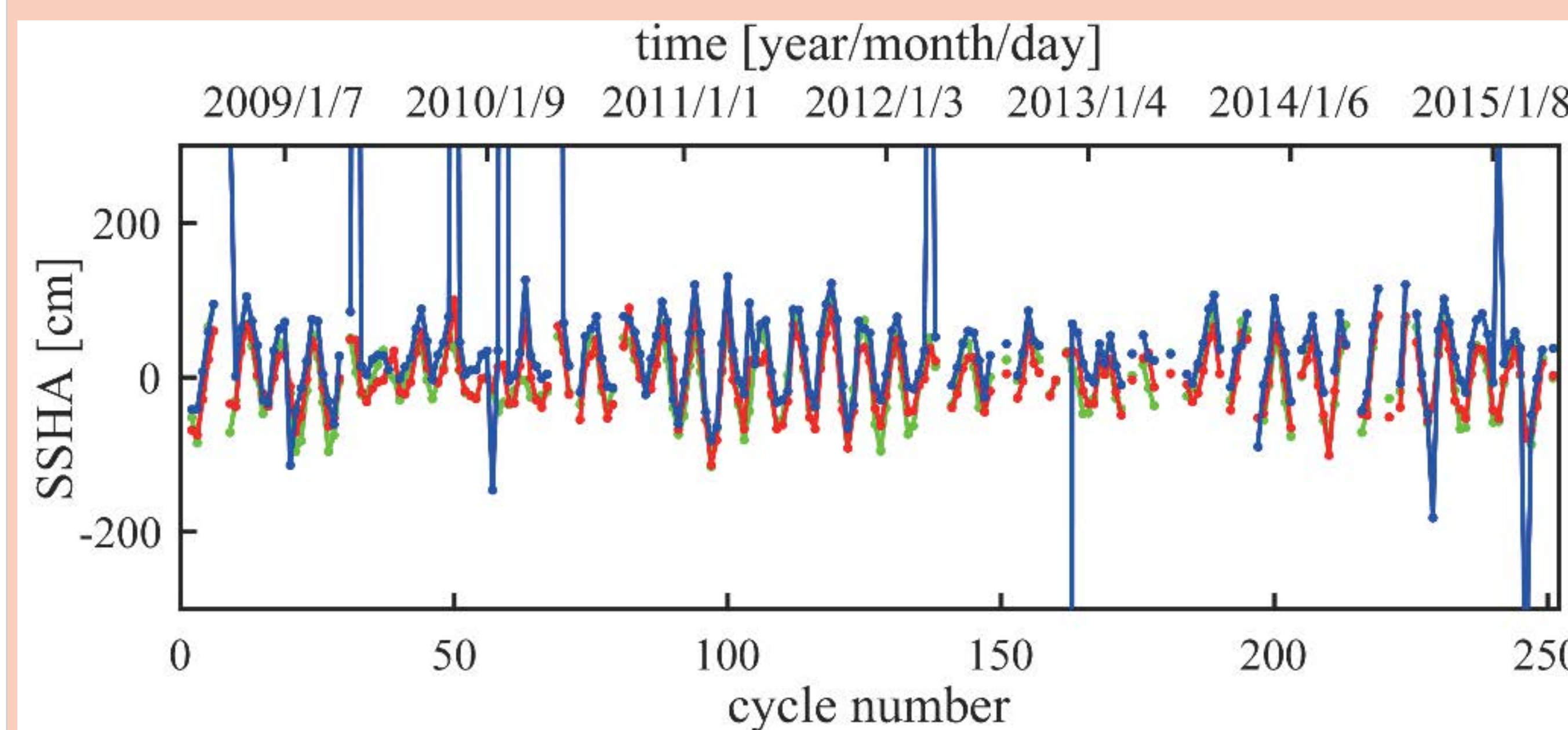


**Fig.8** Time series of the SSHA at 34.21N for tide gauge (green), ALES (blue) and this study (red).

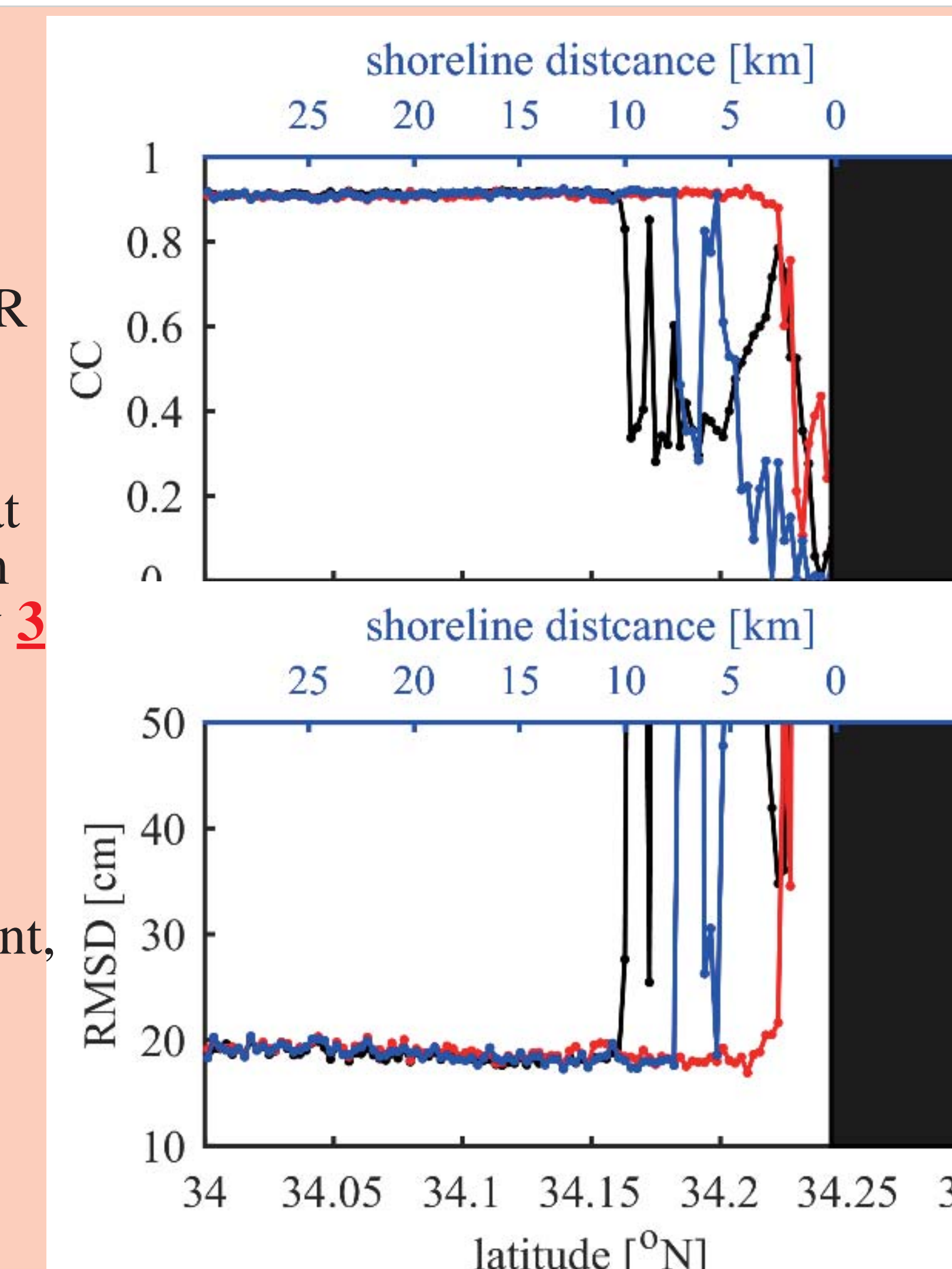


**Fig.7** The correlation coefficient (top) and RMSD (bottom) with the Izuhara tide gauge SSHA for the traditional SGDR (black), ALES (blue) and this study (red). The distance to the shoreline are plotted at the top.

## 4.2 North of Tsushima Island

In the north of Tsushima Island, the approach distance to the shoreline becomes **13 km** for SGDR, and **7 km** for ALES and **this method** (Fig. 9).

Bright parabolas from *Mine Bay* (Fig. 10), whose apex locates at 34.41N, affect only the SGDR retracker. However, contaminations from *Asou Bay* affects all retracker.

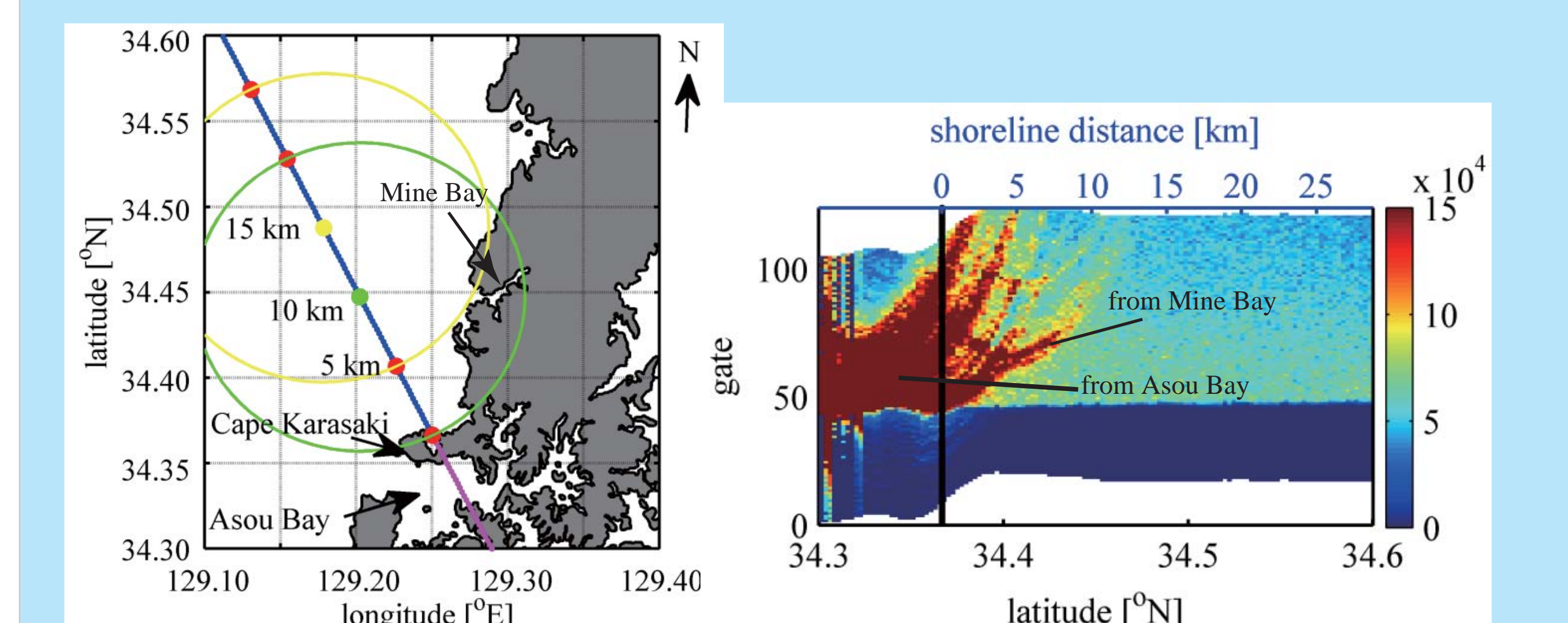


**Fig.9** The RMS of the SSHA for the traditional SGDR (black), ALES (blue) and this study (red) in the area north of Tsushima Island.

**Fig.10** The locations of the Jason-2 track and bays north of Tsushima Island (left panel) and an example of the along-track echogram (cycle 22; right panel).

## 4.3 South of Taiwan

As shown in Fig.3, the shoreline in this study area is smooth w.r.t. Tsushima Island. No significant bright parabola is included in the along-track echograms.

In this case, the approach distance becomes **2 km** for SGDR, **5 km** for ALES and **3 km** for this method (Fig. 11). Performance of the sub-waveform retracker becomes rather worse in this smooth-coast case.

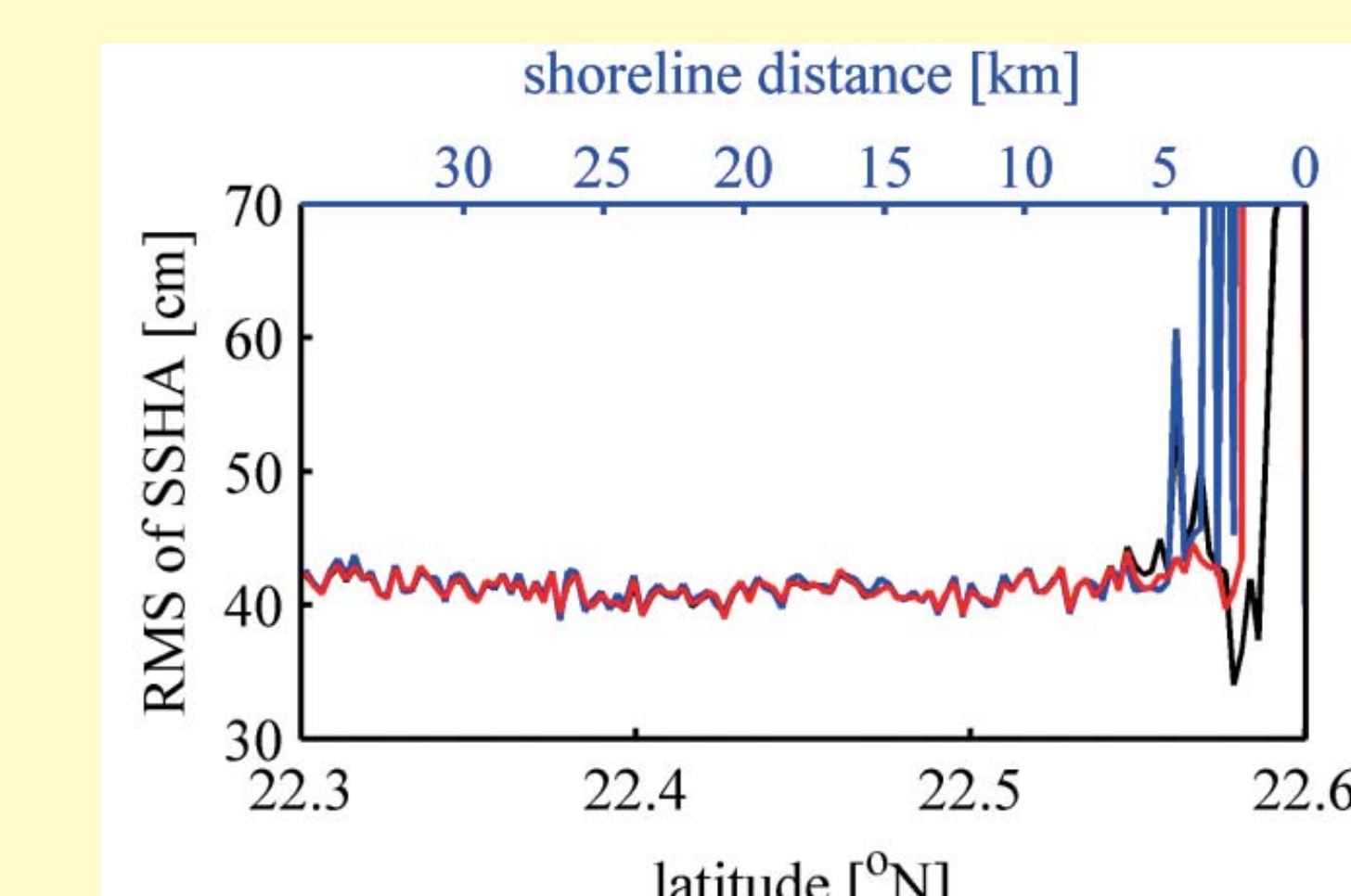


**Fig.11** The RMS of the SSHA for the traditional SGDR (black), ALES (blue) and this study (red) in the area south of Taiwan.

# 5. Discussion and Summary

The new coastal post-processing retracker is proposed that uses along-track echograms. Since it can refer adjacent points in eliminating contaminated echos in waveforms, its performance is better than those of single-point retracker.  
 The SSH can be retrieved as close as **3 km** from the shoreline, even semi-closed bays are present at off-track locations. On-track bays, however, contaminate waveform near the leading edge, and thus no retracker works correctly.

## References

Passaro *et al.* (2014) *Rem. Sen. Env.*, **145**, 173-189, 10.1016/j.res.2014.02.008.  
 Wang and Ichikawa (2017) *Rem. Sens.*, **9**, 762, doi:10.3390/rs9070762.  
 Wessel and Smith (1996) *J.G.R.*, **101**(B4), 8741-8743.